

# Neural Stereoscopic Image Style Transfer

Xinyu Gong<sup>†‡§</sup> Haozhi Huang<sup>†</sup> Lin Ma<sup>†</sup> Fumin Shen<sup>†‡</sup> Wei Liu<sup>†</sup>

<sup>†</sup>Tencent AI Lab <sup>‡</sup>UESTC

{neoxygong, huanghz08, forest.linma, fumin.shen}@gmail.com  
wliu@ee.columbia.edu

## Abstract

Neural style transfer is an emerging technique which is able to endow daily-life images with attractive artistic styles. Previous work has succeeded in applying convolutional neural network (CNN) to style transfer for monocular images or videos. However, style transfer for stereoscopic images is still a missing piece. Different from processing a monocular image, the two views of a stylized stereoscopic pair are required to be consistent to provide the observer a comfortable visual experience. In this paper, we propose a dual path network for view-consistent style transfer on stereoscopic images. While each view of the stereoscopic pair is processed in an individual path, a novel feature aggregation strategy is proposed to effectively share information between the two paths. Besides a traditional perceptual loss used for controlling style transfer quality in each view, a multi-layer view loss is proposed to enforce the network to coordinate the learning of both paths to generate view-consistent stylized results. Extensive experiments show that, compared with previous methods, the proposed model can generate stylized stereoscopic images which achieve the best view consistency.

## 1. Introduction

With the advancement of technology, more and more novel devices provide people with various visual experiences. Among them, devices provide immersive visual experience is one of the most popular, including virtual reality devices [2], augmented reality devices [5], 3D movie systems [3] and 3D televisions [4]. A common component shared by these devices is the stereo imaging technique, which creates the illusion of depth in a stereo pair by means of stereopsis for binocular vision. In order to pro-

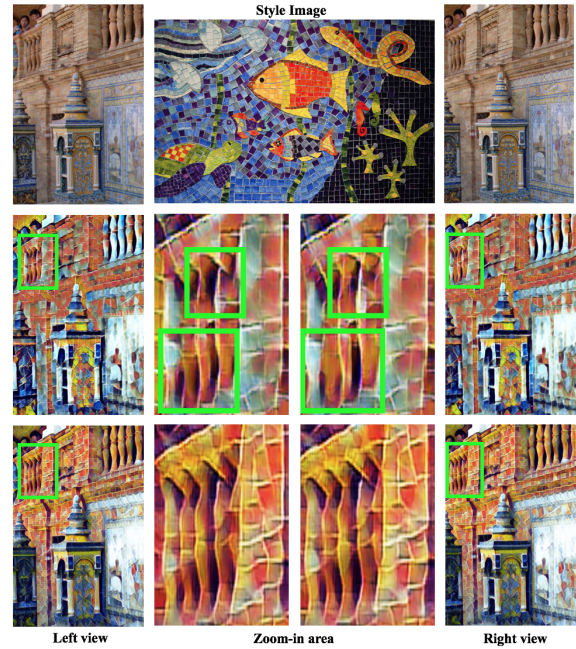


Figure 1. Style transfer applied on stereoscopic images with and without view consistency. The first row shows input stereoscopic images and reference style image. The second row are the stylized results generated by Johnson *et al.*'s method [13]. The middle columns show the zoom-in results, where apparent inconsistency appears in Johnson *et al.*'s method, while our results maintain high consistency.

vide more appealing visual experience, lots of researches strive to apply engrossing visual effects to stereoscopic images [6, 19, 7]. Neural style transfer is one of the emerging technique that can be used to achieve this goal.

Style transfer is a longstanding problem which aims to combine the content of one image with the style of another. Recently Gatys *et al.* [9] revisit this problem and propose an optimization-based solution utilizing features extracted by

<sup>§</sup>Work done while Xinyu Gong was a Research Intern with Tencent AI Lab.

a pre-trained convolutional neural networks, named Neural Style Transfer, which generates the most fascinating results ever. Following this pioneer, lots of efforts have been spent on boosting speed [13, 24], improving quality [25, 28], extending to videos [10, 11, 8] and modeling multiple styles simultaneously [12, 26, 17]. However, the possibility of applying neural style transfer to stereoscopic images has not yet been explored. For stereoscopic images, one straightforward solution is to apply single image style transfer [13] to the left view and the right view separately. However, this method will introduce severe view inconsistency which disturbs the original depth information incorporated in the stereo image pair and brings the observer uncomfortable visual experience [15]. This is because [13] is highly unstable and a slight difference between the input stereo pair may be enormously amplified in the stylized stereo pair. An example is shown in Fig. 1. The first row shows the input stereo pair and the style image. The second row shows the results of [13], where stylized patterns of the same part in the two views are obviously inconsistent.

In the literature of stereoscopic image editing, lots of methods have been proposed to satisfy the need of maintaining view consistency. However, they introduce visible artifacts [21] and require precise stereo matchings [6], while being computationally expensive [19].

In this paper, we propose a dual path convolutional neural network for stereoscopic style transfer, which can generate view-consistent high-quality stylized stereo image pair in real time. Our model takes a pair of stereoscopic images as input simultaneously and stylizes each view of the stereo pair through an individual path. The intermediate features of one path is aggregated with the features from the other path by a trainable feature aggregation block. Besides the traditional perceptual loss used in the style transfer for monocular image [13], a multi-layer view loss is proposed to constrain the stylized outputs of both views to be consistent in multiple scales. With the proposed view loss, our network is able to coordinate the training of both paths and guide the feature aggregation block to learn the optimal feature fusion strategy for generating view-consistent stylized stereo image pair. Compared with previous methods, our method is able to generate stylized results with higher view consistency, while achieving competitive style quality.

In general, the main contributions of our paper are as follow:

- We propose a novel dual path network for stereoscopic style transfer, which can simultaneously stylize a pair of stereoscopic images while maintaining view consistency.
- A multi-layer view loss is proposed to coordinate the training of the two paths of our network, enabling the model to generate view-consistent stylized results.

- A feature aggregation block is proposed to learn the best feature fusion strategy for improving the view consistency of the stylized results.

## 2. Related Work

In this work, we try to generate view-consistent stylized stereo pair via a dual path network, which is closely related to existing literature on style transfer and stereoscopic image editing.

**Neural style transfer.** The first neural style transfer method was proposed by Gatys *et al.* [9], which iteratively optimizes the input image to minimize a content loss and a style loss defined on a pretrained deep neural network. Although this method achieves fascinating results for arbitrary styles, it is time consuming due to the optimization process. Afterwards, models based on feed-forward CNN were proposed to boost the speed [13, 24], which obtain real-time performance without sacrificing too much style quality. Recently, efforts have been spent on extending the single image neural style transfer to videos [22, 12, 8]. The main challenge for video neural style transfer lies in preventing the flicker artifacts brought by temporal inconsistency. To solve this problem, Ruder *et al.* [22] introduced a temporal loss to the time-consuming optimization-based method proposed by Gatys *et al.* [9]. By incorporating temporal consistency to a feed-forward CNN in the training phase, Huang *et al.* [11] was able to generate temporally coherent stylized video in real time. Gupta *et al.* [10] also accomplished real-time video neural style transfer by a recurrent convolutional network trained with a temporal loss. Besides the extensive literature on neural style transfer for images or videos, there is still a short of studies on stereoscopic style transfer. Applying single image style transfer on stereoscopic images directly will cause view inconsistency, which provides the observer an uncomfortable visual experience. In this paper, we propose a dual path network to share information between both views, which can accomplish view-consistent stereoscopic style transfer.

**Stereoscopic image editing** The main difficulty of stereoscopic image editing lies in maintaining the view consistency. Basha *et al.* [6] successfully extended single image seam carving to stereoscopic images, by considering visibility relations between pixels. A patch-based synthesis framework was presented by Luo *et al.* [19] for stereoscopic images, which proposed a joint patch-pair search to enhance the view consistency. Lee *et al.* [16] proposed a layer-based stereoscopic image resizing method, leveraging image warping to handle view correlation. In [21], Northam *et al.* proposed a view-consistent stylization method for simple image filters, but introducing severe artifacts due to layer-wise operations. The above methods are either task specific or time-consuming, which are not able to generalize

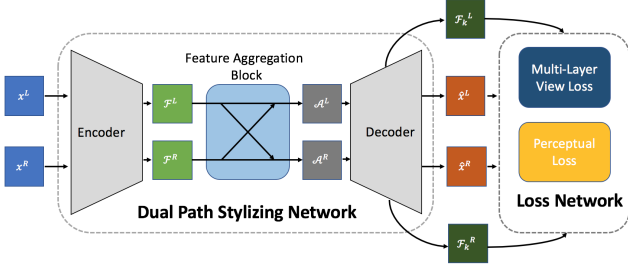


Figure 2. An overview of our model, which consists of a dual path stylizing network and a loss network. The dual path stylizing network takes a pair of stereoscopic images  $x^L, x^R$  as input, generating corresponding stylized images  $\hat{x}^L, \hat{x}^R$ .  $s$  is the reference style image. A feature aggregation block is proposed to share information between dual path. The loss network calculates perceptual loss and multi-layer view loss to guide the training of the stylizing network.

to the style transfer problem. In this paper, we incorporate view consistency in the training phase of a dual path convolutional neural network, which generates view-consistent style transfer results with very high efficiency.

### 3. Method

Generally, our model is composed of two parts: a dual path stylizing network and a loss network (see Fig. 2). The dual path stylizing network takes a stereo pair and processes each view in an individual path. A feature aggregation block is embedded into stylizing networks to effectively share feature level information between the two paths. The loss network computes a perceptual loss and a multi-layer view loss to coordinate the training of both paths of the stylizing network for generating view-consistent stylized results.

#### 3.1. Dual Path Stylizing Network

Our stylizing network can be divided into three parts: an encoder, a feature aggregation block and a decoder. The architecture of the stylizing network is shown in Fig. 3. For simplicity, we mainly illustrate the stylizing process of the left view, which is identical to that of the right view. First, the encoder, which is shared by both paths, takes the original images as input and extracts initial feature maps  $\mathcal{F}^L$  and  $\mathcal{F}^R$  for both views. Second, in the feature aggregation block,  $\mathcal{F}^L$  and  $\mathcal{F}^R$  are combined together to formulate an aggregated feature map  $\mathcal{A}^L$ . Finally,  $\mathcal{A}^L$  is decoded to generate the stylized image of the left view  $\hat{x}^L$ .

##### 3.1.1 Encoder

Our encoder consists of three *Conv* blocks, which down-samples the input images progressively to extract corresponding features. The architecture of the encoder is

Table 1. Encoder Configuration.

Layer	Kernel	Stride	$C_{in}$	$C_{out}$	Acitvation
Conv	$3 \times 3$	1	3	16	ReLU
Conv	$3 \times 3$	2	16	32	ReLU
Conv	$3 \times 3$	2	32	48	ReLU

shown in Table 1. We use *Conv* to denote Convolution-BatchNorm-Activation block.  $C_{in}$  and  $C_{out}$  denote the channel numbers of the input and the output respectively.

##### 3.1.2 Feature Aggregation Block

As aforementioned, separately applying single image style transfer algorithm on each view of a stereo image pair will cause view inconsistency. Thus, we introduce a feature aggregation block to integrate features of both paths, enable our model to exploit more information from both views to preserve view consistency.

The architecture of feature aggregation block is shown in Fig. 4. Taking the original stereoscopic images and the features extracted by the encoder as input, the feature aggregation block outputs an aggregated feature map  $\mathcal{A}^L$ , which contains information of both views.

Specifically, a disparity map is predicted by a pretrained disparity sub-network. The predicted disparity map is used to warp the initial right-view feature map  $\mathcal{F}^R$  to align with the initial left-view feature map  $\mathcal{F}^L$ , obtaining the warped right-view feature map  $W'(\mathcal{F}^R)$ . Explicitly learning a warp operation in this way can reduce the complexity of extracting pixel correspondence information for the model. However, instead of directly concatenating the warped right-view feature map  $W'(\mathcal{F}^R)$  with the initial left-view feature map  $\mathcal{F}^L$ , a gate sub-network is adopted to learn a gating operation for guiding the refinement of  $W'(\mathcal{F}^R)$  generating the refined right feature map  $\mathcal{F}_r^R$ . Finally, we concatenate  $\mathcal{F}_r^R$  with  $\mathcal{F}^L$  along the channel axis to obtain the aggregated feature map  $\mathcal{A}^L$ .

**Disparity sub-network.** Disparity sub-network takes the concatenation of both views of the stereoscopic pair as input, and outputs the estimated disparity map. It is pretrained on the *Driving* dataset [20] in a supervised way, which contains ground-truth disparity maps. To predict the disparity map for the left view, both views of the stereoscopic pair are concatenated along the channel axis to formulate  $\{x^R, x^L\}$ , which thereafter is fed into the disparity sub-network. Similarly,  $\{x^R, x^L\}$  is the input for predicting the right disparity map. The specific architecture of our disparity sub-network is shown in the appendix.

**Gate sub-network.** A gate sub-network is proposed to generate gate map for guiding the refinement of  $W'(\mathcal{F}^R)$ . First, using bilinear interpolation, we resize the input stereoscopic pair  $x^L, x^R$  to the same resolution as the initial left-view

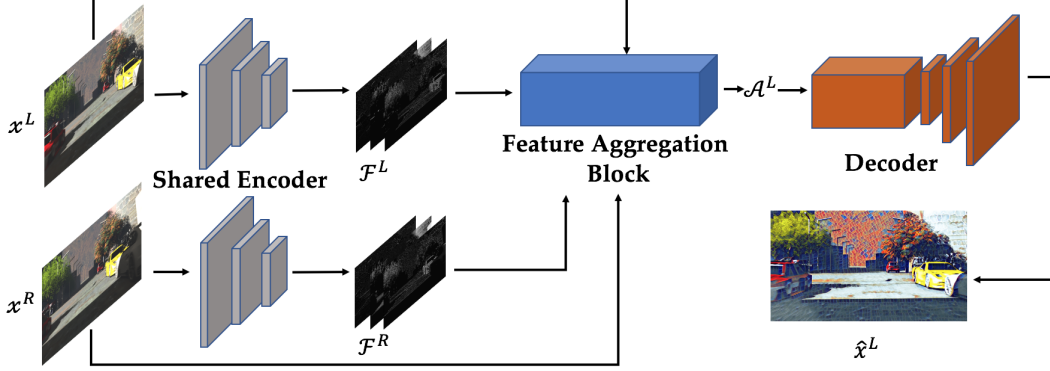


Figure 3. The architecture of stylizing network, composed of an encoder, a feature aggregation block and a decoder. Input images  $x^L$  and  $x^R$  are encoded to feature map  $\mathcal{F}^L$  and  $\mathcal{F}^R$ . Feature aggregation block takes  $\mathcal{F}^L$  and  $\mathcal{F}^R$  as input and aggregates them into  $\mathcal{A}^L$ . Then  $\mathcal{A}^L$  is decoded to stylized result  $\hat{x}^L$ .

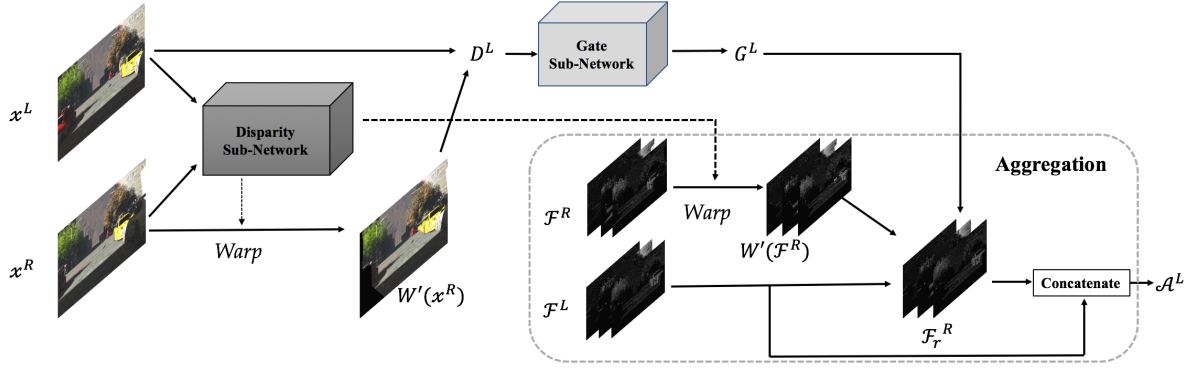


Figure 4. The architecture of the feature aggregation block. The feature aggregation block takes the input stereo pair,  $x^L$ ,  $x^R$ , and corresponding encoder outputs  $\mathcal{F}^L$ ,  $\mathcal{F}^R$ , outputs the aggregated feature map  $\mathcal{A}^L$ . Feature aggregation block is composed of three key components: a disparity sub-network, a gate sub-network and a aggregation.

feature map  $\mathcal{F}^L$ , which is denoted as  $r(x^L)$  and  $r(x^R)$ . Then we calculate the absolute difference between  $r(x^L)$  and  $W'(r(x^R))$ :

$$D^L = |r(x^L) - W'(r(x^R))|. \quad (1)$$

Taking  $D^L$  as input, the gate sub-network predicts a single channel gate map  $G^L$ , which has the same resolution with  $\mathcal{F}^L$ . The range of the pixel value lies in  $[0, 1]$ , which will be used to refine the warped right-view feature map  $W'(\mathcal{F}^R)$  feature maps later. The specific architecture of the gate sub-network is shown in the appendix.

**Aggregation.** Under the guidance of the gate map generated by the gate sub-network, we refine the warped right-view feature map  $W'(\mathcal{F}^R)$  with the initial left-view feature map  $\mathcal{F}^L$  to generate a refined right-view feature map:

$$\mathcal{F}_r^R = W'(\mathcal{F}^R) \odot G^L + \mathcal{F}^L \odot (1 - G^L), \quad (2)$$

where  $\odot$  denotes element-wise multiplication. In our experiments, we find that concatenate  $W'(\mathcal{F}^R)$  with  $\mathcal{F}^L$  directly

to formulate the final aggregated left-view feature map  $\mathcal{A}^L$  will cause ghost artifacts in the stylized results. This is because the mismatching between  $\mathcal{F}^L$  and  $W'(\mathcal{F}^R)$ , which is caused by occlusion and inaccurate disparity prediction, will incorrectly introduce right-view information to the left view. Using the gating operation can avoid this problem. Finally, the refined right-view feature map  $\mathcal{F}_r^R$  is concatenated with the initial left-view feature map  $\mathcal{F}^L$  to formulate the aggregated left-view feature map  $\mathcal{A}^L$ .

### 3.1.3 Decoder

The decoder takes aggregated feature map  $\mathcal{A}^L$  as input, and decode it into stylized images. Note that the decoder is shared by both views. The specific model configuration of the decoder is shown in Table 2. *Res* denotes the Residual block, following a similar configuration to [13]. *Deconv* denotes Deconvolution-InstanceNorm-Activation block.



Table 2. Decoder Configuration.

Layer	Kernel	Stride	$C_{in}$	$C_{out}$	Activation
Conv	$3 \times 3$	1	96	96	ReLU
Conv	$3 \times 3$	1	96	48	ReLU
Res $\times 5$			48	48	ReLU
Deconv	$3 \times 3$	0.5	48	32	ReLU
Deconv	$3 \times 3$	0.5	32	16	ReLU
Conv	$3 \times 3$	1	16	3	tanh

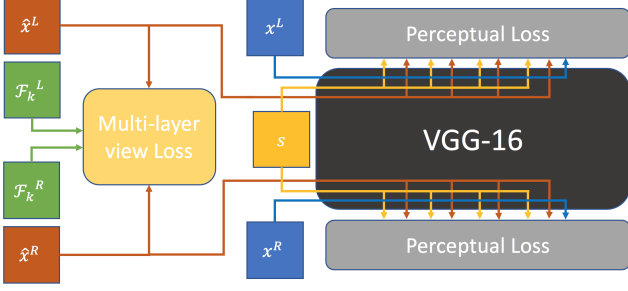


Figure 5. The architecture of the loss network. The perceptual losses of the two views are calculated separately, while the multi-layer view loss is calculated based on the outputs and the features of both views.

### 3.2. Loss Network

Different from the single image style transfer [13], the loss network of our method serves for two purposes. One is to evaluate the style quality of the outputs, and the other is to enforce our network to incorporate view consistency in the training stage. Thus, our loss network calculates a perceptual loss and a multi-layer view loss to guide the training of the stylizing network:

$$\mathcal{L}_{\text{total}} = \sum_{d \in \{L, R\}} \mathcal{L}_{\text{perceptual}}(s, x^d, \hat{x}^d) + \lambda \mathcal{L}_{\text{view}}(\hat{x}^L, \hat{x}^R, \mathcal{F}_k^L, \mathcal{F}_k^R), \quad (3)$$

where  $\mathcal{F}_k$  denotes the  $k$ -th layer feature map of the decoder in the stylizing network. The architecture of our loss network is shown in Fig. 5. While the perceptual losses of the two views are calculated separately, the multi-layer view loss is calculated based on the outputs and the features of both views. By training with the proposed losses, the stylizing network learns to coordinate the training of both paths to leverage the information from both views for generating visually appealing and view-consistent results.

#### 3.2.1 Perceptual Loss

We adopt the definition of the perceptual loss in [13], which has been demonstrated being effective in neural style transfer. The perceptual loss is employed to evaluate the style

quality of the outputs, which consists of a content loss and a style loss:

$$\mathcal{L}_{\text{perceptual}}(s, x^d, \hat{x}^d) = \alpha \mathcal{L}_{\text{content}}(x^d, \hat{x}^d) + \beta \mathcal{L}_{\text{style}}(s, \hat{x}^d). \quad (4)$$

where  $\alpha, \beta$  are the trade-off weights. We adopt a pretrained VGG-16 network [23] to extract features for calculating the perceptual loss.

The content loss is introduced to preserve the high-level content information of the inputs:

$$\mathcal{L}_{\text{content}}(x^d, \hat{x}^d) = \sum_l \frac{1}{H^l W^l C^l} \|\mathcal{F}^l(x^d) - \mathcal{F}^l(\hat{x}^d)\|_2^2, \quad (5)$$

where  $\mathcal{F}^l$  denotes the feature map at layer  $l$  in VGG-16 network.  $W^l, H^l, C^l$  are the height, width and channel size of the feature map at layer  $l$  respectively. The content loss constrains the feature maps of  $x^d$  and  $\hat{x}^d$  to be similar, where  $d = \{L, R\}$  represents different views.

The style loss is employed to evaluate style quality of the generated images. Here we use the Gram matrix as the style representation, which has been demonstrated to be effective in [9]:

$$G_{ij}^l(x^d) = \frac{1}{H^l W^l} \sum_h \sum_w \mathcal{F}^l(x^d)_{h,w,i} \mathcal{F}^l(x^d)_{h,w,j}, \quad (6)$$

where  $G_{ij}^l$  denotes the  $i, j$ -th element of the Gram matrix of the feature map at layer  $l$ . The style loss is defined as the mean square error between the Gram matrices of the output and the reference style image:

$$\mathcal{L}_{\text{style}}(s, \hat{x}^d) = \sum_l \frac{1}{C^l} \|G^l(s) - G^l(\hat{x}^d)\|_2^2. \quad (7)$$

Matching the Gram matrices of feature maps has also been demonstrated to be equivalent to minimizing the Maximum Mean Discrepancy (MMD) between the output and the style reference [18].

#### 3.2.2 Multi-layer View Loss

Besides a perceptual loss, a novel multi-layer view loss is proposed to encode view coherence into our model in the training phase. The definition of the multi-layer view loss is:

$$\mathcal{L}_{\text{view}} = \mathcal{L}_{\text{view}}^{\text{img}} + \mathcal{L}_{\text{view}}^{\text{feat}}. \quad (8)$$

While the image-level view loss constrains the outputs to be view-consistent, the feature-level view loss constrains the feature maps in the stylizing network to be consistent. The image-level view loss is defined as:

$$\mathcal{L}_{\text{view}}^{\text{img}} = \frac{1}{\sum_{i,j} M_{i,j}^L} \|M^L \odot (\hat{x}^L - W(\hat{x}^R))\|_2^2 + \frac{1}{\sum_{i,j} M_{i,j}^R} \|M^R \odot (\hat{x}^R - W(\hat{x}^L))\|_2^2. \quad (9)$$

where  $M$  is the per-pixel confidence mask of disparity map, which has the same shape with stylized images. The value of  $M_{i,j}$  is either 0 or 1, where 0 in mismatched area, and 1 in well-matched corresponding area.  $\hat{x}^L$  and  $\hat{x}^R$  are stylized results. We use  $W$  to denote the warp operation using the ground-truth disparity map, provided by the Scene Flow Datasets [20]. Thus,  $W(\hat{x}^L)$  and  $W(\hat{x}^R)$  are warped stylized stereo pair, using the ground truth disparity map.

In order to enhance view consistency of stylized images further, we also enforce corresponding activation value on intermediate feature maps of left and right content images to be identical. Thus, feature-level view loss is introduced. Similarly, feature-level view loss is defined as follow:

$$\begin{aligned} \mathcal{L}_{\text{view}}^{\text{feat}} = & \frac{1}{\sum_{i,j} m_{i,j}^L} \|m^L \odot [\mathcal{F}_k^L - W(\mathcal{F}_k^R)]\|_2^2 \\ & + \frac{1}{\sum_{i,j} m_{i,j}^R} \|m^R \odot [\mathcal{F}_k^R - W(\mathcal{F}_k^L)]\|_2^2. \end{aligned} \quad (10)$$

where  $m$  is the resized version of  $M$ , sharing the same width and height with  $k$ -th layer's feature map in decoder.  $\mathcal{F}_k^L$  and  $\mathcal{F}_k^R$  are the feature map fetched out from  $k$ -th layer in stylizing network. Similarly,  $W(\mathcal{F}_k^L)$  and  $W(\mathcal{F}_k^R)$  are the warped feature map using ground truth disparity map.

## 4. Experiment

### 4.1. Detailed Implementation

We use *Driving* in the Scene Flow Datasets [20] as our dataset, which contains 4.4k pairs of stereoscopic images. 440 pairs of them are used as testing samples, while the rest are used as training samples. The loss network (VGG-16) is pretrained on the image classification task [23]. Note that during the training phase, the multi-layer view loss is calculated using the ground-truth disparity map provided by the Scene Flow Datasets [20] to warp fetched feature maps and stylized images. Specifically, we fetch feature maps at 7-th layer of decoder to calculate feature-level view loss.

The disparity sub-network is trained for 2 epochs and fixed thereafter. Then, we train the other parts of the stylizing network for 2 epochs. We set  $\alpha = 1$ ,  $\beta = 500$ ,  $\lambda = 100$ . The batch size is set to as 1. The learning rate is fixed as  $1e - 3$ . For optimization we use Adam [14]. Our model takes about 1.01 seconds to generate a stylized stereo pair with a single NVIDIA Tesla M40 GPU.

### 4.2. Qualitative Results

We apply the trained model to some stereoscopic pictures from Flickr [1] to show the visual qualities of different styles. In Fig. 6, stylized results in four different styles are presented, from which we can see that the semantic content of the input images are preserved, while the texture

and color are transferred from the reference style images successfully. Besides, view consistency is also maintained. Please refer to the supplementary material for more visual results.

### 4.3. Comparison

In this section, we compare our method with the single image style transfer method [13]. Though there are many alternative baseline designed for single image neural style transfer, both of them will suffer from similar view inconsistency artifacts as Johnsons method [13]. Hence, we only choose [13] as a representative. Also, we testify the effectiveness of the multi-layer view loss and the feature aggregation block.

As the evaluation metric, we define a term called the mean view loss  $MVL$ :

$$MVL = \frac{1}{N} \sum_{n=1}^N \mathcal{L}_{\text{view}}^{\text{img}}(I_n), \quad (11)$$

where  $N$  is the total number of test images,  $I_n$  is the  $n$ -th image in the test dataset,  $\mathcal{L}_{\text{view}}^{\text{img}}$  is the image-level view loss defined in Equation 9. In other words,  $MVL$  is employed to evaluate the average of the image-level view losses over the whole test dataset. Similarly, we also define mean style loss ( $MSL$ ) and mean content loss ( $MCL$ ):

$$MSL = \frac{1}{N} \sum_{n=1}^N \mathcal{L}_{\text{style}}(I_n) \quad (12)$$

$$MCL = \frac{1}{N} \sum_{n=1}^N \mathcal{L}_{\text{content}}(I_n) \quad (13)$$

For clarity, the single image style transfer method is named as *SingleImage*, where the single image method trained with image-level view loss is named as *SingleImage-IV*. Our full model with a feature aggregation block trained with a multi-layer view loss is named as *Stereo-FA-MV*. The variant model trained without the multi-layer view loss is named as *Stereo-FA*. The variant model with a feature aggregation block but trained with an image-level view loss is named as *Stereo-FA-IV*. We evaluate the  $MVL$ ,  $MSL$  and  $MCL$  of the above models across four styles: *Fish*, *Mosaic*, *Candy* and *Dream*. In Tab. 3, we can see that the mean view loss  $MVL$  of our full model *Stereo-FA-MV* is the smallest. The result of the single image style transfer method is the worst. Comparing *Stereo-FA-IV* with *SingleImage-IV*, we know that the feature aggregation block benefits the view consistency. Comparing *Stereo-FA-MV* with *Stereo-FA-IV*, we find that constraining the view loss in the feature level besides the image level improves the view consistency further. According to the value of  $MSL$  and  $MCL$  in Tab. 3, we can also observe that minimizing



Figure 6. The visual results of our proposed stereoscopic style transfer method. While the high-level contents of the inputs are well preserved, the style details are successfully transferred from the style images. Meanwhile, view consistency is primarily maintained.

Table 3. *MVL*, *MSL* and *MCL* of five different methods over 4 styles. Our proposed method achieves the best performance in *MVL*.

Models	<i>MVL</i>	<i>MSL</i>	<i>MCL</i>
<i>SingleImage</i>	2861	282	509309
<i>SingleImage-IV</i>	1127	397	489493
<i>Stereo-FA</i>	2751	<b>246</b>	484973
<i>Stereo-FA-IV</i>	1037	342	482664
<i>Stereo-FA-MV</i>	<b>1014</b>	417	<b>445336</b>

the view loss inevitably impedes the decrease of style loss, while it can preserve more content information.

In order to give a more intuitive comparison, we visualize the view inconsistency maps of the single image style transfer method and our proposed method in Fig. 7. The view inconsistency map is defined as:

$$V = \sum_c (\hat{x}_c^L - W(\hat{x}^R)_c) \odot M^L \quad (14)$$

where  $\hat{x}_c^L$  and  $W(\hat{x}^R)_c$  denote  $c$ -th channel of  $\hat{x}^L$  and  $W(\hat{x}^R)$  respectively. Note that  $W$  denotes the warp operation using the ground truth disparity map, provided by the Scene Flow Datasets [20]. Compared with our method, a large number of white pixels can be observed in the results of *SingleImage*, which indicates that our method can preserve the view consistency better.

Moreover, a user study is conducted to compare *SingleImage* with our method. Specifically, a total number

of 21 participants take part in our experiment. Ten stereo pairs are randomly picked up from the Waterloo-IVC 3D database [27]. For each of the stereo pair, we apply style transfer using three different style images (*candy*, *mosaic*, *fish*, *mosaic*). As a result,  $3 \times 10$  stylized stereoscopic pairs are generated. Each time, a participant is shown the stylized results of the two methods on a 3D TV with a pair of 3D glasses and asked to vote for the preferred one (which is more view-comfortable). Specifically, the original stereo pairs are shown before the stylized results of the two methods, in order to give participants the correct sense of depth as references. The final results is shown in Fig. 8. 73% votes are voted to the stylized results generated by our method, which demonstrates that our method achieves better view consistency and provides more satisfactory visual experience.

#### 4.4. Ablation Study on Feature Aggregation

To testify the effectiveness of the proposed feature aggregation block, we set up an ablation study. Our feature aggregation block consists of three key components: warping, gating and concatenation. We test 4 variant models with different settings of these key components for obtaining the final aggregated feature maps  $\mathcal{A}^L$  and  $\mathcal{A}^R$ . For simplicity, we only describe the process of obtaining  $\mathcal{A}^L$ .

In the first model *CON*,  $\mathcal{A}^L$  is obtained by concatenating  $\mathcal{F}^R$  with  $\mathcal{F}^L$ . In the second model *W-CON*,  $\mathcal{A}^L$  is obtained





Figure 7. Visualization of the view inconsistency. The second row shows the view inconsistency maps of the single image style transfer method [13]. The third row shows our results. There are less number of white pixels in our results, which indicates that our results are more view-consistent.

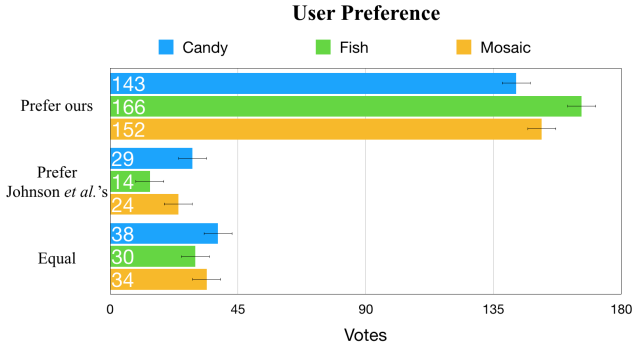


Figure 8. The user preference result. Three styles are used in our experiment. In total, 630 votes are collected. While our results receive 461 votes, Johnson *et al.*'s single image style transfer results receive 67 votes.

by concatenating  $W'(\mathcal{F}^R)$  with  $\mathcal{F}^L$ . In the third model  $W-G$ , we use the refined feature map  $\mathcal{F}_r^R$  as  $\mathcal{A}^L$  directly. In the last model  $W-CON-G$ ,  $\mathcal{A}^L$  is obtained by concatenating  $\mathcal{F}_r^R$  with  $\mathcal{F}^L$ , which is the proposed architecture of our feature aggregation block. (Note that Stereo-FA is equal to  $W-CON-G$  in our paper) For eliminating the affect of the multi-layer view loss, all models above are trained with the perceptual loss only, using *Fish*, *Mosaic*, *Candy* and *Dream* as the reference style images.

Tab. 4 shows the mean view loss of the 4 variant models. Comparing  $CON$  with  $W-CON$ , we can see that concatenating  $W'(\mathcal{F}^R)$  with  $\mathcal{F}^L$  outperforms concatenating  $\mathcal{F}^R$  with  $\mathcal{F}^L$  directly. This is because that  $W'(\mathcal{F}^R)$  is aligned with  $\mathcal{F}^L$  along channel axis, which relieves the need of learning pixel correspondences. Comparing  $W-CON$  with  $W-CON-G$ ,  $W-CON-G$  achieves better performance, which indicates

Table 4.  $MVL$ ,  $MSL$  and  $MCL$  of four different feature aggregation blocks. Our proposed feature aggregation block architecture has the best result in  $MVL$ .

Models	$MVL$	$MSL$	$MCL$
$CON$	3628	260	500801
$W-CON$	2941	<b>240</b>	486489
$W-G$	3219	244	503298
$W-CON-G$	<b>2751</b>	246	<b>484973</b>

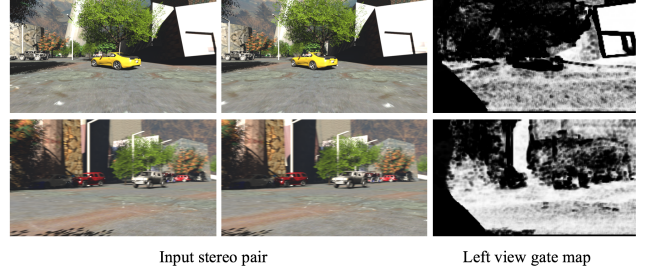


Figure 9. The visualization of gate maps. The left and middle column is the input stereo pair. The right column shows the left view gate map generated by gate sub-network.

that gating operation does refine  $W'(\mathcal{F}^R)$ . Compared with  $W-CON-G$ ,  $W-G$  has a larger mean view loss, which demonstrates that the concatenated skip connection is essential.

Recalling the Equation 2, the refined feature map  $\mathcal{F}_r^R$  is a linear combination of the initial feature map  $\mathcal{F}^L$  and the warped feature map  $W'(\mathcal{F}^R)$ , under the guidance of the gate map. In order to give an intuitive understanding of the gate maps, we visualize several gate maps in Fig.9. For simplicity, we only illustrate the gate maps for the left view. Generated gate maps are shown in the right column. The black regions in the gate maps indicate the mismatching between  $\mathcal{F}^L$  and  $W'(\mathcal{F}^R)$ . Here, the mismatching is caused by occlusion and inaccurate disparity estimation. For the mismatched areas, the gate map learns to predict 0 values to enforce the refined feature map  $\mathcal{F}_r^R$  directly copy values from  $\mathcal{F}^L$  to avoid inaccurately incorporating information from the right view.

## 5. Conclusion

In this paper, a novel dual path network was proposed to deal with style transfer on stereoscopic images. While each view of an input stereo pair is processed in an individual path to transfer the style from a reference image, a novel feature aggregation block is proposed to propagate the information from one path to another. To coordinate the learning of both paths for acquiring better view consistency, a multi-layer view loss was proposed to constrain the stylized outputs of both views to be consistent in multiple scales. Extensive experiments demonstrated that our method is able to generate stylized results with better view consistency compared to previous methods.



## References

- [1] Flickr. <https://www.flickr.com>.
- [2] HTC Vive. <https://www.vive.com/us/>.
- [3] IMAX Corporation. <https://www.imax.com>.
- [4] LG 4K HDR Smart TV. <http://www.lg.com/us/tvs/lg-OLED65G6P-oled-4k-tv>.
- [5] Microsoft HoloLens. <https://www.microsoft.com/en-gb/hololens>.
- [6] T. Basha, Y. Moses, and S. Avidan. Geometrically consistent stereo seam carving. In *Proceedings of ICCV*, 2011.
- [7] C.-H. Chang, C.-K. Liang, and Y.-Y. Chuang. Content-aware display adaptation and interactive editing for stereoscopic images. *IEEE Transactions on Multimedia*, 13(4):589–601, 2011.
- [8] D. Chen, J. Liao, L. Yuan, N. Yu, and G. Hua. Coherent online video style transfer. In *Proceedings of ICCV*, 2017.
- [9] L. A. Gatys, A. S. Ecker, and M. Bethge. Image style transfer using convolutional neural networks. In *Proceedings of CVPR*, 2016.
- [10] A. Gupta, J. Johnson, A. Alahi, and L. Fei-Fei. Characterizing and improving stability in neural style transfer. In *Proceedings of ICCV*, 2017.
- [11] H. Huang, H. Wang, W. Luo, L. Ma, W. Jiang, X. Zhu, Z. Li, and W. Liu. Real-time neural style transfer for videos. In *Proceedings of CVPR*, 2017.
- [12] X. Huang and S. Belongie. Arbitrary style transfer in real-time with adaptive instance normalization. In *Proceedings of ICCV*, 2017.
- [13] J. Johnson, A. Alahi, and L. Fei-Fei. Perceptual losses for real-time style transfer and super-resolution. In *Proceedings of ECCV*, 2016.
- [14] D. Kingma and J. Ba. Adam: A method for stochastic optimization. *arXiv preprint arXiv:1412.6980*, 2014.
- [15] F. L. Kooi and A. Toet. Visual comfort of binocular and 3d displays. *Displays*, 25(2):99–108, 2004.
- [16] K.-Y. Lee, C.-D. Chung, and Y.-Y. Chuang. Scene warping: Layer-based stereoscopic image resizing. In *Proceedings of CVPR*, 2012.
- [17] Y. Li, C. Fang, J. Yang, Z. Wang, X. Lu, and M.-H. Yang. Diversified texture synthesis with feed-forward networks. *arXiv preprint arXiv:1703.01664*, 2017.
- [18] Y. Li, N. Wang, J. Liu, and X. Hou. Demystifying neural style transfer. *arXiv preprint arXiv:1701.01036*, 2017.
- [19] S.-J. Luo, Y.-T. Sun, I.-C. Shen, B.-Y. Chen, and Y.-Y. Chuang. Geometrically consistent stereoscopic image editing using patch-based synthesis. *IEEE transactions on visualization and computer graphics*, 21(1):56–67, 2015.
- [20] N. Mayer, E. Ilg, P. Häusser, P. Fischer, D. Cremers, A. Dosovitskiy, and T. Brox. A large dataset to train convolutional networks for disparity, optical flow, and scene flow estimation. In *Proceedings of CVPR*, 2016.
- [21] L. Northam, P. Asente, and C. S. Kaplan. Consistent stylization and painterly rendering of stereoscopic 3d images. In *Proceedings of NPAR*, 2012.
- [22] M. Ruder, A. Dosovitskiy, and T. Brox. Artistic style transfer for videos. In *Proceedings of GCPR*, 2016.
- [23] K. Simonyan and A. Zisserman. Very deep convolutional networks for large-scale image recognition. *arXiv preprint arXiv:1409.1556*, 2014.
- [24] D. Ulyanov, V. Lebedev, A. Vedaldi, and V. S. Lempitsky. Texture networks: Feed-forward synthesis of textures and stylized images. In *Proceedings of ICML*, 2016.
- [25] D. Ulyanov, A. Vedaldi, and V. Lempitsky. Instance normalization: The missing ingredient for fast stylization. *arXiv preprint arXiv:1607.08022*, 2016.
- [26] H. Wang, X. Liang, H. Zhang, D.-Y. Yeung, and E. P. Xing. Zm-net: Real-time zero-shot image manipulation network. *arXiv preprint arXiv:1703.07255*, 2017.
- [27] J. Wang, A. Rehman, K. Zeng, S. Wang, and Z. Wang. Quality prediction of asymmetrically distorted stereoscopic 3d images. *IEEE Transactions on Image Processing*, 24(11):3400–3414, 2015.
- [28] X. Wang, G. Oxholm, D. Zhang, and Y.-F. Wang. Multi-modal transfer: A hierarchical deep convolutional neural network for fast artistic style transfer. In *Proceedings of CVPR*, 2017.